Impact of Surface Modification on Cellular Uptake and Cytotoxicity of Silica Nanoparticles

Sandra Vranic
Tokyo University of Science
Eri Watanabe
Tokyo University of Science
Kayoko Miyakawa
Tokyo University of Science
Sakie Takeuchi
Tokyo University of Science
Yurika Osada
Tokyo University of Science
Sahoko Ichihara
Jichi Medical University
Cai Zong
Tokyo University of Science
Wenting Wu
Nagoya University
Toshihiro Sakurai
Tokyo University of Science
Akira Sato
Tokyo University of Science
Yasushi Hara
Tokyo University of Science
Toshihiro Suzuki
Tokyo University of Science
Ryo Abe
Tokyo University of Science
Sonja Boland
University of Paris
Lang Tran
Institute of Occupational Medicine
Gaku Ichihara (gak@rs.tus.ac.jp)
Tokyo University of Science https://orcid.org/0000-0001-5707-5300

Research

Keywords: Silica nanoparticles (SiO2 NPs), cytotoxicity, cellular uptake, Silicon dioxide

Posted Date: October 27th, 2020

DOI: https://doi.org/10.21203/rs.3.rs-96205/v1

Abstract

Background: Silica nanoparticles (SiO_2 NPs) are widely used in industrial products as additives for rubber and plastics or as filler strengthening concrete, as well as being used in the biomedical field for drug delivery and theranostic purposes. The present study investigated the effects of amino or carboxyl functionalization of rhodamine-labeled SiO_2 NPs on cellular uptake and cytotoxicity.

Methods: Male mice were randomly divided into seven groups (n=6, each) and exposed to non-functionalized (plain), carboxyl or amino-functionalized rhodamine-labeled SiO_2 NPs at 2 or 10 mg/kg bw, or endotoxin-free water, by pharyngeal aspiration. At 24 hours after administration, the mice were euthanized and bronchoalveolar lavage fluid (BALF) was collected for differential cell count and identification of silica nanoparticle uptake using confocal microscopy. In the *in vitro* studies, murine RAW264.7 macrophages were exposed to non-functionalized, amino- or carboxyl-functionalized Rhodamine-labeled SiO_2 NPs. Nonspecific caspase inhibitor and necrostatin-1 were used to determine the involvement of caspase or receptor-interacting protein 1 kinase domain in the cytotoxicity.

Results: The *in vivo* study demonstrated that the neutrophil and macrophage counts and the percentage of macrophages with internalized particles was highest in the order of carboxyl >= amino- > > non-functionalized particles. The *in vitro* study demonstrated greater cytotoxicity for non-functionalized silica nanoparticles, compared to the others. Treatment with non-specific caspase or necroptosis inhibitor did not attenuate MTS cytotoxicity of non-functionalized silica nanoparticles.

Conclusion: We conclude that carboxyl-functionalzed SiO_2 NPs are internalized by macrophages more efficiently but less cytotoxic than plain SiO_2 NPs. The cytotoxic effect of plain SiO_2 NPs, which cannot be explained by apoptosis or necroptosis, can be avoided by carboxyl- or amino- functionalization.

Introduction

Nanoparticles (NPs) can be potentially used in various applications in the fields of nanotechnology, research and medicine. The small particle size and unique chemical and physical properties are highly exploitable in different consumer products as well as in the biomedical field, such as drug delivery vectors, imaging purposes and/or cell tracking [1–4]. However, their low biodegradability, potential inhalation or prolonged skin contact with nanoparticles based on the small diameter and high surface reactivity are considered drawbacks for wider usage [4]. Therefore, before the application of NPs becomes widely accepted, it is necessary to establish their toxicological profile and understand the potential adverse effects that might arise from human and environmental, accidental or desired exposure.

Silicon dioxide (silica) nanoparticles (SiO_2 NPs) are nowadays widely used in industrial products as additives for rubber and plastics or as strengthening fillers for concrete. In addition, they are used in the biomedical field for drug delivery or theranostic purposes [5–9]. The toxicological profile of SiO_2 NPs has been widely studied recently, with increasing body of literature on the potential adverse effects of SiO_2 NP

exposure. Silica materials exist in both crystalline and amorphous forms. The most common form of crystalline silica is quartz, whose toxicity has been studied for many years and is linked with chronic bronchitis, emphysema and silicosis [9–11]. Compared to the crystalline SiO_2 NPs, the amorphous form is less toxic [5, 6]. With regard to the mechanism of toxicity, *in vitro* studies have shown that the toxic effect of SiO_2 NPs is mainly mediated by induction of oxidative stress and activation of intrinsic or mitochondrial (caspase-activated) apoptotic pathways [12–17]. Reactive oxygen species (ROS)-mediated cell death is considered one of the main mechanisms of action of many different types of nanomaterials (NMs), including silica NPs. In contrast, the results of a recent study indicate that total silanol content, cell membrane damage, and cell viability mediate the toxicity of SiO_2 NPs, rather than intracellular ROS [18]. The majority of the *in vivo* toxicological data are based on acute exposure studies, which usually include intra-tracheal instillation, intravenous injection or oral exposure [5, 6]. Submicron amorphous silica particles were found to have greater inflammatory and cytotoxic potential compared to their bigger counterparts [19]. In the study of Morris et al. [20], C57BL/6 mice were intratracheally instilled with 4 or 20 mg SiO_2 NPs/kg body weight and significant effects were observed only at the high dose of 20 mg/kg. Twenty hours after instillation, approximately 20- and 10-fold increase in the cell number was observed in the bronchoalveolar lavage (BAL) of mice treated with the bare and amine-coated SiO_2 NPs, respectively, compared to the control mice; neutrophils were also increased about 30- and 20-fold, respectively [20]. Other studies demonstrated acute and chronic exposure to SiO_2 NPs aggravated airway inflammation [21–25].

One of the strategies to build “safe by design” NPs is to apply various types of surface modifications to coat the NPs and modulate their surface reactivity, thereby decreasing their toxic effects. For example, surface modification of SiO_2 NPs was found to reduce their aggregation and nonspecific binding [26], while functionalization with amino or phosphate groups was shown to mitigate their pro-inflammatory and immunomodulatory effects in allergic airway inflammation [21]. Interestingly, coating of SiO_2 NPs with polyethylene glycol polymer (PEG) was not found to be efficient in reducing the pro-inflammatory potential of these NPs *in vivo* [21, 27]. Furthermore, few *in vitro* studies have shown that surface modification of SiO_2 NPs reduces their potential for inflammasome activation and cytotoxicity [28, 29].

With this in mind, the present study was designed to determine the effect of surface modification of 25 nm amorphous SiO_2 NPs both *in vivo* (C57BL/6JJcl mice) and *in vitro* (murine macrophage RAW 264.7 cell line), with a special emphasis on their pro-inflammatory and cytotoxic potentials. Our data support the hypothesis that surface modification of SiO_2 NPs can modulate the uptake properties of the material, their pro-inflammatory potential and cytotoxicity. We showed that exposure to bare SiO_2 NPs with terminal Si-OH group decreased the number of macrophages collected from bronchoalveolar lavage fluid (BALF) *in vivo*. On the other hand, both carboxyl- and amino-functionalized SiO_2 NPs were efficiently taken up by macrophages or neurtrophils *in vivo*, accompanied by increase in the number of neutrophils collected from BALF at the high dose used (10 mg NPs/kg bw). The results showed that SiO2 NPs cytotoxicity is not related with internalization of SiO2 NPs and neutrophil infiltration, although

internalization of SiO2 NPs might be linked to neutrophil infiltration. The results of *in vitro* and *in vivo* experiments were complementary to each other, underlining the importance of surface modification of SiO_2 NPs in modulating their toxicological profile, and suggesting that functionalization of 25 nm SiO_2 NPs with carboxyl groups in consumer products or for biomedical applications could lead to efficient cellular uptake, and that functionalization with the amino or carboxyl group reduced the toxicity of SiO_2 NPs.

Materials And Methods

Silica nanoparticles

Rhodamine-labeled SiO_2 NPs, “Sicastar“, of 30 nm in diameter, functionalized with carboxy (Cat. #40-02-301), amino group (Cat. #40-01-301) or non-functionalized (Cat. #40-00-301) were purchased from Micromod Partikeltechnologie, Rostock, Germany. All NPs were dispersed in water at 25 mg/mL. The size of the NPs in water or in complete cell culture medium was characterized by DLS, Zeta potential analysis and TEM. Zeta-potential was measured with Photal LEZA-600 (Otsuka Denshi Co., Osaka). The fluorescence intensities of the three types of silica NPs were measured at different concentrations using ARVO^{TM}MX 1420 Multilabel Counter (Perkin Elmer, Waltham, MA). The slopes of the regression lines for independent variable of concentration and dependent variable of fluorescence intensity were calculated to obtain the relative fluorescence intensity between different types of silica NPs labeled with rhodamine (Supplementary file 1).

Animals

Forty-two male C57BL/6JJcl mice of 7-week-old were purchased from CLEA Japan Inc (Tokyo, Japan). All mice were housed and acclimatized to the new environment for one week in a pathogen-free animal room controlled at 23–25 °C and 55–60% humidity. Light was set within a 12-h light-dark cycle (on at 09:00 and off at 21:00), and food and water were provided *ad libitum*. This study was conducted according to the Japanese law on the protection and control of animals and the Animal Experimental Guidelines of Tokyo University of Science. The experimental protocol was also approved by the Animal Ethics Committee of Tokyo University of Science prior to the experiment.

Mice were randomly divided into seven groups of six each and exposed to plain SiO_2 NPs, carboxyl SiO_2 NPs or amino SiO_2 NPs at 2 or 10 mg/kg bw, which were equivalent to 40 or 200 μg per mouse if body weight was 20 g, or endotoxin-free water. These exposure levels were half of those adopted in a previous study, which demonstrated that exposure to SiO_2 NPs by intratracheal instillation increased the number of macrophages in BALF at 0.5 mg silica/mouse (20 mg/kg bw) but not at 0.1 mg silica/mouse (4 mg/kg bw) (Morris 2016). With regard to the relation of the above exposure levels by intratracheal instillation to those by inhalation, one study showed that 690 μg of titanium dioxide deposited in the rat lung after exposure to ultrafine titanium dioxide at 125 mg/m^3 for 2 hours (Osier 1997). Since the alveolar surface areas of rat and mice are 2970 [30] and 82.2 cm^2 [31], respectively, the estimated lung deposition of

titanium dioxide in mice was 690 × 82.2/2970 = 19 μg when exposed to ultrafine titanium dioxide at 125 mg/m^3 for 2 hours. The higher dose of 200 μg in the present study is comparable to ultrafine particles deposited in the lungs after inhalation exposure to ultrafine particles at 125 mg/m^3 for 21 hours. SiO_2 NPs dispersed in water at 25 mg/mL were vortexed and then further diluted with endotoxin-free water to obtain the NP solution at 1 and 5 mg/mL.

Mice were anesthetized with pentobarbital and then exposed to 40-μl aliquot of samples of SiO_2 NPs by pharyngeal aspiration, as described previously (Gabazza et al. 2004, Wu et al. 2015). The technique of pharyngeal aspiration involved placement of the nanoparticle suspension on the back of the tongue followed by pulling of the tongue to induce a reflex gasp with resultant aspiration of the droplets. At 24 h after administration, the mice were euthanized by intraperitoneal injection of pentobarbital. BAL was performed by cannulation of the trachea with 18-gauge needle, and infusion and collection of 5/6 mL of saline was repeated six times.

Total and differential cell counts in BALF

The recovered BALF was centrifuged (1,500 rpm, 5 min, 4 °C), and the cell pellet was mixed with 1 mL of ACK lysing buffer (Gibco-Thermo Fischer Scientific, Waltham, MA) for hemolysis. Ten mL of Dulbecco's phosphate buffer saline (DPBS) was added and centrifuged at 1,500 rpm and 4 °C. The resultant pellet was re-suspended in DPBS for total and differential cell counts. The total cell count was measured using hematocell counter. Aliquots of 5×10^4 cells in 400 μl DPBS per slide were prepared for cytospins. The cell mixture was added to EZ Single Cytofunnel®(Thermo, UK and centrifuged for 10 min at 1,000 rpm with Cytospin, using cytoslides. The slides were dried overnight at room temperature and then stained with the Differential Quik Stain Kit (Modified Giemsa, Sysmex Co., Kobe, Japan) for differential cell count in 10 fields (20 x magnification) of each slide.

Fluorescence immunocytology

A slide obtained by Cytospin was washed in DPBS three times and incubated with blocking agent (1% BSA) for one hour. The slide was further incubated with Biotin anti-Ly6G and Ly6C (Gr-1) (BD, Franklin Lakes, NJ), which was diluted 400 folds in 1% BSA, for one hour at room temperature, washed in DPBS three times and then incubated with 200-fold diluted Cy5 streptavisin (BioLegend, San Diego, CA) for 30 min at room temperature to stain the neutrophils. Ly6G and Ly6C (Gr-1) were used as markers of neutrophils, as their expression levels are known to correlate with differentiation and maturation of granulocytes [32, 33] and are only expressed transiently on bone marrow cells in the monocyte lineage [33]. The slides were counterstained with Hochest33342 for 10 min at room temperature and enclosed with Fluorescent Mounting Media (Dako, Agilent, Santa Clara, CA). Cells and SiO_2 NPs were observed with confocal microscope Fv10i (Olympus, Tokyo)

Cell culture

Murine macrophages RAW 264.7 cell were kindly provided by Prof. Kenneth Dawson, University of College Dublin and grown in Dulbecco's Modified Eagle Medium (DMEM, high glucose) with L-glutamine and

phenol red (Wako, Cat. #044-29765) supplemented with 1 mM sodium pyruvate (100 mM, Gibco, Cat. #11360-070), 100 U/mL penicillin, 100 mg/mL streptomycin and 250 ng/mL amphotericin B (anti-anti, Gibco, Cat #15240-062), 2 mM glutamine and 10% FBS. All experiments were performed with cells from passages 4 to 15. Cells were grown in T25-flasks (Violamo, AS ONE Co., Osaka) in monolayers. Exponentially growing cells were maintained in a humidified atmosphere of 5% CO_2 and 95% air at 37 °C and were passaged once every two days using a cell scraper (NEST 100071).

NP treatment

Depending on the experiment and after reaching 70–80% confluence, the cells were seeded onto appropriate cell culture plates and treated with silica nanoparticles of different surface modification. Before exposure to NP, the cells were rinsed with PBS to eliminate trace amounts of FBS. Treatments were performed under FBS-free condition for two reasons: *1)* serum is reported to modulate NP uptake [34], and *2)* to mimic *in vivo* condition whereby bronchial cells are not directly exposed to serum proteins. Stock of 30 nm rhodamine-labeled silica nanoparticles (25 mg/mL in water) was vortexed shortly before the preparation of the final dilution for the treatment.

MTS assay

MTS assay was conducted using CellTiter 96® Aqueous One Solution Cell Proliferation Assay (Promega, Madison, WI) as described previously [35] and the instructions provided by the manufacturer. Briefly, RAW264.7 cells were seeded at 1.5×10^4 cells/well onto 96-well plates and incubated at 37 ºC in a humidified atmosphere of 5% CO_2 and 95% air for 24 hours. After incubation, the cell culture medium was removed from each well with a multichannel pipette, and the cells were washed three times with DPBS to remove FBS. The cells were incubated for 4 or 24 hours with the three types of silica nanoparticles dispersed in FBS-free cell culture medium at a final concentration ranging from 0.3 to 30 μg/cm^2. After incubation with the silica nanoparticles, the cells were washed twice with 1xDPBS, and incubated with MTS reagent (1.4 mL CellTiter 96® AQueous One Solution Reagent and 7.1 mL of complete phenol red-free cell culture medium with FBS). Cellular viability was determined by measuring absorbance at 490 nm, which reflected the reduction of {3-(4,5-dimethylthiazol-2-yl)-5-(3-carboxymethoxyphenyl)-2-(4-sulfophenyl)-2H-tetrazolium} (MTS) to formazan by mitochondria in viable cells.

Confocal microscopy

Cells were seeded in 8 well Lab-TekIITM chambered cover glasses (Nunc, Thermo Scientific, Dominique Dutscher, Brumath, France) at 16,590 cells/well in complete cell culture medium, and then incubated for 24 h. Upon 70–80% confluence, the cells were washed three times with DPBS to remove FBS and treated with 0.3 mL/well of NPs at pre-selected concentrations for 24 h at 37 °C and 5% CO_2. After removal of medium, the cells were washed one time and fixed in 4% PFA for 20 min at 25 °C, rinsed twice with DPBS and then incubated with Cell Mask Green Plasma Membrane Stain (C37608 Thermo Fisher Science, Waltham, MA) and Hoechst for 10 min. The cells were washed with DPBS twice. After embedding the cells in Mounting Medium, they were observed by confocal microscopy (model FV.10, Olympus, Tokyo). The maximum concentration of silica nanoparticles 35.2×10^5 μg/cell (8.40 μg/cm^2) was determined to

be equivalent to exposure level of 40 μg/mouse *in vivo*, given that the average number of macrophages collected in BALF was 1.14×10^5 cells/mouse.

Flow cytometry

RAW264.7 cells were seeded onto 6-well plates at 2.37×10^4 cells/cm^2 in complete cell culture medium and incubated for 24 h before treatment. After treatment with 3.0 mL/well of silica NPs at the preselected concentrations for 1 or 4 h in dark, the medium was removed, cultures were thoroughly washed with PBS three times and treated with 0.1% trypan blue for 1 min to quench the fluorescence of rhodamine on the cell surface. The concentration of trypan blue for quenching the fluorescence of rhodamine was determined beforehand by plot of trypan blue and rhodamine intensity in RAW264.7 cells exposed to bare rhodamine-labeled SiO_2 NPs (Supplementary Fig. 2). The cells were washed with PBS, mixed with 500 μL of FACS buffer (PBS containing 0.5% FBS and 0.1% NaN_3) and harvested by cell scraper. Cell-associated fluorescence was detected using FACSCalibur™ and results were analyzed with FlowJo software (BD, Franklin Lakes, NJ). The Mean Fluorescence Intensity (MFI) of rhodamine (excitation 488 nm, Filter range 564–606 nm) from three different size fractions indicated by the forward scatter (FS) was shown by the flow cytometer. The results are reported as the median of the distribution of cell fluorescence intensity obtained by analyzing cells in the gate. To adjust the differences in the fluorescence intensity relative to weight, the intensity of rhodamine fluorescence was measured at different concentrations of three types of SiO_2 NPs using ARVOMx-fla system (485 nm/535 nm 1.0 s).

LDH cytotoxicity assay

LDH cytotoxicity assay was conducted using Pierce LDH cytotoxicity assay kit following the instructions provided by the manufacturer (Thermo Fisher Scientific). Briefly, RAW264.1 cells were plated at 10^4 cells/well in 100 μl of medium in a 96-well tissue culture plate. To minimize the cytotoxic effect of lack of FBS, DMEM was replaced by Opti-MEM for LDH cytotoxicity assay and further investigation of the effect of pan-caspase or necroptosis inhibitor. After incubation at 37 ºC under 5% CO_2 for 24 hours, the cells were exposed to bare, carboxyl-functionalized, amino-functionalized rhodamine-labeled SiO_2 NPs at 5.85 μg /cm^2 (19.5 μg/mL). After the exposure for 1, 4, 12, 24, 36 and 48 hours, the supernatant of the culture medium was collected by centrifugation, and dispensed at 50 μl/well into another 96-well plate. Each cell was incubated in the presence of 50 μl of LDH reaction mixture at room temperature for 30 min in dark. The reaction was stopped by adding 50 μl of stop solution, and absorbance at 490 and 680 nm was read by Plate reader Gen5 (BioBik, Osaka, Japan).

Evaluation of effects of caspase inhibitor Z-VAD-FMK

Z-VAD-FMK, {Benzyloxycarbonyl-L-valyl-L-alanyl-[(2*S*)-2-amino-3-(methoxycarbonyl)propionyl]}fluoromethane, cell-permeable pan-caspase inhibitor was dissolved at 20 mM in DMSO and diluted to 20 or 40 μM by culture medium Opti-MEM® | Reduced Serum Media (Thermo Fisher Scientific). RAW264.1 cells were preincubated with Z-VAD-FMK at 20 or 40 μM or vehicle for one hour, and exposed to plain rhodamine-labeled silica nanoparticles at 28 μg/mL for 18 hours in

Opti-MEM®. Cytotoxicity was evaluated using CellTiter 96® Aqueous One Solution Cell Proliferation Assay (Promega, Madison, WI) as mentioned above.

Evaluation of effects of necroptosis inhibitor necrostatin-1

Necrostatin-1 or necrostatin-1 inactive control (Cayman Chemical, Ann Arbor, MI) was dissolved in 20 mM in DMSO and diluted to 10 or 20 μM by culture medium Opti-MEM® | Reduced Serum Media (Thermo Fisher Scientific). Raw264.1 cells were preincubated with Z-VAD-FMK at 10 or 20 μM or vehicle for one hour, and exposed to plain rhodamine-labeled silica nanoparticles at 8.4 μg/cm^2 (28 μg/mL) for 18 hours in Opti-MEM®. Cytotoxicity was evaluated using CellTiter 96® Aqueous One Solution Cell Proliferation Assay (Promega, Madison, WI) as mentioned above.

Quantitative real time PCR

RAW264.1 cells were seeded onto 6-well plates at 23,700 cells/cm^2 and exposed to silica NPs at the concentration of 0.33, 1.67 and 8.37 μg/cm^2 (1.06, 5.30, and 26.50 μg/mL, respectively). The cells were collected by centrifugation at 1,000 rpm for 5 min at 4ºC. Total RNA from the cells was isolated by using ReliaPrepTM RNA Cell Miniprep System (Promega, Fitchburg, WI). The concentration of total RNA was quantified by spectrophotometry (ND-1000; NanoDrop Technologies, Wilmington, DE). RNA was reverse transcribed to single-strand cDNA using SuperScript III First-Strand Synthesis System for RT-PCXR (Life Technologies). The cDNA was subjected to quantitative PCR analysis with Thunderbird cyber green master mix (TOYOBO, Osaka, Japan) and primers designed by TAKARA (Kusatsu, Japan). The primers are 5’-GTCCCTCAACGGAAGAACCAA-3’ (forward) and 5’-TCTCAGACAGCGAGGCACAT-3’ (reverse) for MIP-2, 5’-GATCGGTCCCCAAAGGGATG-3’ (forward) and 5’-GTGGTTTGTGAGTGTGAGGGT-3’ (reverse) for TNFα and 5’-GATCATTGCTCCTCCTGAGC-3’ (forward) and 5’-ACTCCTGCTTGCTGATCCA-3’ (reverse) for β-actin.

Statistical analysis

Data are expressed as mean ± standard deviation (SD). Differences with the control or between groups were analyzed respectively by Dunnett’s or Tukey’s multiple comparison following one-way ANOVA. A probability (p) of < 0.05 denoted the presence of a statistically significant difference. For the analysis of relative fluorescence intensity among different types of particles, regression lines were obtained by forcing the intercept to zero using Excel 2016 (Microsoft, Redmond, WA). All statistical analyses were performed using JMP (version 14, SAS Institute, Cary, NC).

Results

Physicochemical properties of SiO_2 NPs

We studied first the *in vitro* and *in vivo* effects of the three types of 25 nm SiO_2 NPs. For this purpose, we used plain SiO_2 NPs with hydroxyl group (OH-SiO_2 NPs), and carboxyl- or amino-modified SiO_2 NPs

(COOH- SiO_2 NPs or NH_2- SiO_2 NPs). The diameter and surface charge of these NPs were determined by DLS and Zeta potential measurements both in water (since the materials were dispersed in endotoxin-free, ultra-pure water for intra-tracheal instillation in mice lungs) and in the cell culture medium relevant to the exposure of RAW264.8 cells. As indicated in Table 1, the mean diameters of the carboxyl and amino modified, and OH-SiO_2 NPs in water were 33.9 ± 0.1 nm, 34.8 ± 0.2 nm and 34.1 ± 0.2 nm, respectively, indicating a mono-dispersed size distribution of NPs. Similarly, the mean diameters of the three types of SiO_2 NPs in the cell culture medium were comparable, with 33.6 ± 0.6, 33.6 ± 0.3 and 36.3 ± 0.3 nm for the carboxyl and amino modified, and plain NPs, respectively. Interestingly, regardless the surface modification of these NPs using three different functional groups, their overall surface charge was neither modified in water nor in the cell culture medium (Table 1). As indicated, the mean surface charges of COOH-, NH_2- and OH-SiO_2 NPs in water were − 25.6 ± 4.05, -41.5 ± 3.02 and − 33.2 ± 1.85 mV, respectively, while the respective values in the cell culture medium were − 23.5 ± 4.0 mV, -23.8 ± 2.5 mV and − 23.3 ± 1.9, respectively. That the mean surface charge was more negative than − 20 mV indicates good colloidal stability of SiO_2 NPs both in water and in the cell culture medium.

Table 1
Physicochemical properties of SiO_2 NPs dispersed in water and in complete cell culture medium, studied by DLS and Zeta potential measurement.

Type of SiO_2 NPs	Solvent	Diameter (nm)	Zeta potential (mV)
NH_2-SiO_2 NPs	Water	33.9 ± 0.1	-25.6 ± 4.05
COOH-SiO_2 NPs	Water	34.8 ± 0.2	-41.5 ± 3.02
OH-SiO_2 NPs	Water	34.1 ± 0.2	-33.2 ± 1.85
NH_2-SiO_2 NPs	FBS-free medium	33.6 ± 0.6	-23.5 ± 3.96
COOH-SiO_2 NPs	FBS-free medium	33.6 ± 0.3	-23.8 ± 2.54
OH-SiO_2 NPs	FBS-free medium	36.3 ± 0.3	-23.3 ± 1.87
Data are mean ± SD of 4 and 3 measurements of diameter and zeta potentials, respectively.			

In vivo toxicity

In order to address the *in vivo* toxicity of the three types of SiO_2 NPs, we measured body and lung weights of the test animals as a rough indication of disturbance of body and lung homeostasis following instillation of NPs. We also collected BALF for total and differential cell counts, which are reliable markers of lung inflammation induced by NPs. In order to better understand the localization of NPs after the

instillation procedure, the macrophages and neutrophils were differentially stained and examined by confocal microscopy.

Body and lung weight

There was no significant difference in body weight between vehicle-treated control mice and mice treated with any of the three types of SiO_2 NPs at 2 or 10 mg NPs/kg bw (Table 2). On the other hand, there was a significant increase in the lung weight in the OH-SiO_2NP -treated mice at 2 and 10 mg/kg bw.

Table 2
Weight of body and lungs of mice at 24 h after exposure to SiO2NP by pharyngeal aspiration.

	Concentration of SiO_2 NPs (mg/kg bw)	n	Body weight (g)	Lung weight (mg)
Vehicle	0	6	20.9 ± 1.4	293 ± 22
NH_2-SiO_2 NPs	2	6	21.6 ± 0.4	301 ± 5
	10	6	21.3 ± 1.4	321 ± 23
COOH-SiO_2 NPs	2	6	21.6 ± 1.2	305 ± 16
	10	6	21.5 ± 1.0	322 ± 6
OH-SiO_2 NPs	2	6	21 ± 1	324 ± 25*
	10	6	20 ± 1	331 ± 16*
*P < 0.05, compared with the vehicle control, by Dunnett's multiple comparison following ANOVA.				

Table 3
MIP-2 mRNA level relative to β-actin in RAW264.1 cells exposed to different SiO2NPs.

	n	Concentration of SiO_2 NPs (μg/cm^2)			
		0	**0.33**	**1.67**	**8.34**
3 h exposure					
Vehicle	3	0.33 ± 0.11			
NH_2- SiO_2 NPs	3		0.54 ± 0.17	1.02 ± 0.09	2.40 ± 0.11
COOH- SiO_2 NPs	3		0.61 ± 0.20	0.89 ± 0.16	1.61 ± 0.15
OH-SiO_2 NPs	3		0.40 ± 0.07	1.82 ± 0.48	166 ± 30*
6 h exposure					
Vehicle	3	0.04 ± 0.01			
NH_2- SiO_2 NPs	3		0.05 ± 0.01	0.16 ± 0.09	0.55 ± 0.11
COOH- SiO_2 NPs	3		0.08 ± 0.02	0.18 ± 0.01	0.53 ± 0.12
OH-SiO_2 NPs	3		0.09 ± 0.06	1.65 ± 0.29	25 ± 29*
*P < 0.05, compared with the vehicle control, by Dunnett's multiple comparison following ANOVA.					

Table 4
TNF-α mRNA level relative to β-actin in RAW264.1 cells exposed to different SiO_2 NPs.

	n	Concentration of SiO_2 NPs (μg/cm^2)			
		0	0.33	1.67	8.34
3 h exposure					
Vehicle	3	3.1 ± 1.3			
NH_2-SiO_2 NPs	3		4.2 ± 0.7	7.3 ± 3.2	7.3 ± 3.3
COOH-SiO_2 NPs	3		5.3 ± 3.3	8.9 ± 5.0	11.2 ± 1.5
OH-SiO_2 NPs	3		3.6 ± 0.8	5.2 ± 1.4	28.3 ± 9.3*
6 h exposure					
Vehicle	3	0.28 ± 0.14			
NH_2-SiO_2 NPs	3		0.33 ± 0.06	0.36 ± 0.10	1.42 ± 0.42
COOH- SiO_2 NPs	3		0.33 ± 0.11	0.68 ± 0.17	1.64 ± 0.33*
OH-SiO_2NP	3		0.36 ± 0.10	1.57 ± 1.29*	0.63 ± 0.55
*P < 0.05, compared with the vehicle control, by Dunnett's multiple comparison following ANOVA.					

BALF total and differential cell count

Treatment with different types of SiO_2 NPs at 2 mg/kg bw did not increase the total cell number (Fig. 1A). On the other hand, treatment with amino- and carboxyl-functionalized SiO_2 NPs at 10 mg/kg bw induced increase in BALF total cell count. Interestingly, there was no change in the total cell number after treatment with hydroxyl functionalized SiO_2 NPs at 10 mg /kg bw. Further analysis showed treatment with 10 mg/kg bw OH-SiO_2 NPs decreased the total number of BALF macrophages, compared to the untreated group (Fig. 1B). On the other hand, 10 mg/kg bw carboxyl functionalized SiO_2 NPs increased the number of macrophages (Fig. 1B), and carboxyl- or amino-functionalized SiO_2 NPs increased BALF neutrophils (Fig. 1C). The increase in the numbers of total cells and neutrophils was higher with COOH-SiO_2 NPs than NH_2-SiO_2 NPs (Fig. 1A and C). Hydroxyl (plain) SiO_2 NPs increased the number of neutrophils at 2 mg/kg bw, but had no such effect at 10 mg/kg bw (Fig. 1C).

Interaction of SiO_2 NPs with BALF macrophages and neutrophils

COOH- and NH_2-SiO_2 NPs were both similarly internalized by cells regardless their dose, while only a few OH-SiO_2 NPs made contact with the cells (Fig. 2A). Internalization of NH_2- and COOH-SiO_2 NPs into the macrophages was not influenced by their dose (persistently ~ 60%), while only around 40% of the macrophages internalized OH-SiO_2 NPs (Fig. 2B and D). On the other hand, internalization of carboxyl and amino functionalized SiO_2 NPs into the neutrophils was dose-dependent (30–40% of cells internalized SiO_2 NPs at 10 mg/kg bw, Fig. 2C and E), with the numbers and percentages of such neutrophils significantly higher at 10 mg/kg bw of each of the above two types, compared to those neutrophils with internalized hydroxyl functionalized SiO_2 NPs (only 10% at 10 mg/kg bw).

In vitro toxicity of NPs

MTS cell viability assay of SiO_2 NPs in RAW264.7 macrophage cell line

The MTS assay was used to assess the cytotoxic potential of SiO_2 NPs, in which tetrazolium salts are reduced to formazan by metabolically active cells (probably through NAD(P)H-dependent dehydrogenases), producing measurable color changes proportionate to the number of viable cells. The percentage of live cells is then estimated by measuring absorbance of formazan at 490 nm, wavelength that is clearly distinguishable from rhodamine absorption profile. Treatment of the cells with OH-SiO_2 NPs, but not NH_2- and COOH-SiO_2 NPs, significantly decreased cell viability in time- and dose-dependent manners (Fig. 3). Exposure to OH-SiO_2 NPs significantly decreased cell viability at ≥ 3 μg/cm^2 (≥ 10 μg/ml) after 4 h of treatment and at ≥ 7.5 μg/cm^2 (≥ 25 μg/ml) after 24 h of treatment. The decrease in cell viability was also dose-dependent, with < 40% of the cells remaining metabolically active after 4 h exposure to 30 μg/cm^2 (100 μg/ml) of OH-SiO_2 NPs (Fig. 3A). The decrease in cell viability was also time-dependent; <40% of the cells was still alive and metabolically active after 24 h of treatment with 7.5 μg/cm^2 (25 μg/ml) OH-SiO_2 NPs (Fig. 3B). The above *in vitro* data support the hypothesis that OH-SiO_2 NPs is the most toxic among the three types and suggest that the observed decrease in BALF macrophages (Fig. 1B) was mediated through cell death. Similarly, this cytotoxic effect of OH-SiO_2 NPs could explain the observed increase in BALF neutrophil count, compared to the control, though it but reached a plateau at ≥ 2 mg/kg bw (Fig. 1C), resulting in lack of statistical different in BALF total number of cells in the untreated mice. These data highlight the need to perform BALF differential cell count in order not to overlook subtle effects of these NPs on different cells in the lung.

Interaction of SiO_2 NPs with RAW264.8 macrophage cell line

Next, we assessed the interaction of the three types of NPs with RAW264.8 macrophages in order to understand the mechanism of OH-SiO_2 NPs toxicity. COOH- SiO_2 NPs were efficiently internalized by

RAW264.8 macrophages from 1 h after exposure, in dose- and time-dependent manners (based on the higher amounts of internalized NPs in RAW264.8 macrophages after 4 and 24 h of treatment, Fig. 4A). Interestingly, hydroxyl plain NPs mainly co-localized with the plasma membrane irrespective of the dose used (Fig. 4A). This was remarkable already after 1 h of treatment at the highest concentration of NPs and even more prominent after 4 and 24 h of treatment.

Internalization of NPs by cells was further quantified by flow cytometry (Fig. 4B and Suppl Fig. 1). To eliminate the signal coming from NPs adsorbed on the surface of the cells, 0.1% trypan blue was added shortly before the analysis. The working concentration of trypan blue was optimized prior to the experiment (Suppl Fig. 1). Flow cytometry showed three populations of RAW264.4 cells (Suppl Fig. 2). Due to difference in the slopes of the regression lines, with rhodamine intensity as the dependent variable and SiO_2 NPs concentration as the independent variable (Suppl Fig. 3), the fluorescence of COOH-SiO_2 NPs and OH-SiO_2 NPs was each divided by the ratio of the slope for COOH-SiO_2 NPs and OH-SiO2NPs to the slope for NH_2-SiO_2 NPs for normalization. Exposure to COOH-SiO_2 NPs increased the mean value of the normalized fluorescence intensity in the population gated to A (Fig. 4B), B and C (Suppl Fig. 4) in dose- and time-dependent manners. Exposure to NH_2- or OH-SiO_2 NPs increased the mean of normalized intensity in all examined populations to an extent lesser than exposure to COOH-SiO_2 NPs.

Cytotoxicity of OH-SiO_2 NPs

The LDH cytotoxicity test showed higher LDH release from the cells exposed to OH-NPs compared to the other types of NPs (Suppl Fig. 5). Pretreatment with pan caspase or necroptosis inhibitor did not attenuate the decrease in MTS cell viability induced by exposure to OH-SiO_2 NPs for 18 h (Fig. 5A and B), suggesting that the cytotoxicity of OH-SiO_2 NPs is unrelated to apoptosis or necroptosis.

SiO_2 NPs-induced RAW264.8 macrophage-related pro-inflammatory response

Finally, we assessed the pro-inflammatory potential of the three types of NPs by measuring the expression of two genes by RT-qPCR. At 8.34 μg/cm^2, OH-SiO_2 NPs increased the expression of both MIP-2 genes at 3 and 6 h post-exposure (Table 2). The same NPs also increased the expression of TNF-α at 3 h post-treatment at 8.34 μg/cm^2 and at 6 h post-treatment at 1.67 μg/cm^2. Exposure to at 8.34 μg/cm^2 COOH-SiO_2 NPs also increased the expression of TNF-α at 6 h post-treatment.

Discussion

The results of the *in vivo* study showed that COOH- SiO_2 NPs increased BALF neutrophils to the greatest extent among the three types of SiO_2 NPs. This increase was accompanied by a higher rate of COOH-SiO_2 NPs internalized into BALF neutrophils compared with NH_2- or OH-SiO_2 NPs. On the other hand, OH-SiO_2 NPs reduced the number of BALF macrophages in a dose-dependent manner. In the in vitro arm of the study, we confirmed the uptake of COOH-SiO_2 NPs by RAW 264.7 macrophage cells by flow cytometry,

and that the extent of such uptake was greater than that of NH_2- or plain SiO_2 NPs. Toxicity analysis using the MTS assay and LDH cytotoxicity test showed the highest toxicity of plain SiO_2 NPs among three types of SiO_2 NPs. The cell toxic effect was not accompanied by recovery of cell viability by pan-caspase inhibitor or necroptosis inhibitor, suggesting that the cell death was necrotic in nature. Taking the results of both the *in vivo* and *in vitro* studies together, we can conclude that exposure to OH-SiO_2 NPs induces cell death of macrophages, while exposure to the carboxyl- or amino- modification of SiO_2 NPs reduces the cytotoxicity. Recruitment of neutrophils was the highest by COOH-SiO_2 NPs, whereas OH-SiO_2 NPs induced the mRNA expression of proinflammatory cytokines to a greater extent than COOH-SiO_2 NPs. It is possible that the relatively low recruitment of macrophages and lymphocytes in OH-SiO_2 NPs - treated mice resulted from death of these cells, while exposure to OH-SiO_2 NPs induced a more extensive inflammatory response, as evident by the higher transcription levels of proinflammatory cytokines in the remaining cells and increased lung weight following exposure to OH-SiO_2 NPs.

Flow cytometry showed the uptake of COOH-SiO_2 NPs by RAW264.8 macrophages starting from 1 hr after exposure and was higher than those of NH_2- and OH-SiO_2 NPs. The higher rate of uptake of COOH-SiO_2 NPs is in agreement with our recent study, which showed better interaction of COOH-SiO2 NPs with Caco-2 cells compared with NH_2- and OH-SiO_2 NPs [35].

Confocal microscopy showed localization of OH-SiO_2 NPs in the proximity of the cell membrane and less internalization of these particles in RAW264.8 macrophages. This finding suggests that OH-SiO_2 NPs-induced cell death of RAW264.8 macrophages is not necessarily through internalization of the particles, but rather the physical contact between the particles and cell membrane, in agreement with the recent finding of the cytolytic toxicity of silanol-rich SiO_2 NPs (Spyrogianni et al. 2017).

Increased lung weight can reflect pulmonary inflammation, which is associated with intense protein/fluid leakage from the vasculature into the alveoli mediated by inflammatory signals from pulmonary cells [36]. The results suggests that NH_2- and COOH-SiO_2 NPs can recruit neutrophils only at the high dose of 10 mg/kg bw, with COOH-SiO_2 NPs being more potent in attracting neutrophils, while the lack of dose dependency in increasing the number of neutrophils and the decrease in macrophage numbers with larger dose of OH-SiO_2 NPs could be explained by cell death induced by these NPs. With the aim of confirming and further investigating these findings, we analyzed the uptake of fluorescently-labelled SiO_2 NPs by neutrophils and macrophages and performed *in vitro* experiments using RAW264.8 macrophage cell line.

The different patterns of interaction with the cells and subsequent cellular uptake observed in the present study could perhaps explain the differences in the toxicological profile of the three types of SiO_2 NPs used in this study. While COOH-SiO_2 NPs were efficiently internalized into the cells, OH-SiO_2 NPs predominantly interacted with the cell plasma membrane, potentially damaging the membrane and inducing cell death. The zeta potentials of all types of SiO_2 NPs in water were negative, in the order of

NH_2-SiO_2 NPs, OH-SiO_2 NPs and COOH-SiO_2 NPs. On the other hand, the zeta potentials of all types of SiO_2 NPs in the FBS-free media were almost of the same negative values. These results are in agreement with our recent study, which showed greater interaction of Caco-2 cells or THP-1 cells with COOH-SiO_2 NPs than OH- or NH_2-SiO_2 NPs [35]. The present findings and our previous study show that the difference in the extent of internalization or cytotoxicity is not explained by the differences in zeta potentials. Further studies are needed to understand the mechanism(s) involved in cellular internalization and toxicity of SiO_2 NPs.

Conclusions

Carboxyl modification of SiO2 NPs increases their uptake into macrophages while carboxyl- or amino-modification of SiO_2 NPs reduces cytotoxicity of SiO_2 NPs. The cytotoxicity of OH-SiO_2 NPs could be related to the physical contact between NPs and the cell membrane, though further studies are needed to test this hypothesis and to determine the exact mechanism of SiO_2 NPs-induced cytotoxicity.

Declarations

Ethics approval

This study was conducted according to the Japanese law on the protection and control of animals and the Animal Experimental Guidelines of Tokyo University of Science. The experimental protocol was also approved by the Animal Ethics Committee of Tokyo University of Science prior to the experiment. The approval number is Y14059.

Consent for publication

Not applicable

Availability of data and materials

All date generated or analysed during the current study are included in this published article and its supplementary information files.

Competing interests

The authors declare that they have no competing interests.

Funding

This work was supported by Japan Society for the Promotion of Science (JSPS) International Fellowship for Research in Japan (Short-term Program) #PE13040, JSPS NEXT Program #LS056 and Japan Science and Technology Agency (JST) Strategic Japanese-EU Cooperative Program: Study on managing the potential health and environmental risks of engineered nanomaterials.

Authors' contribution

SV, SI, SB, LT and GI designed the study and interpreted the data. SV, EW, WW and SI conducted animal studies. EW, KM, ST and YO conducted in vitro studies. CZ, TSa, AS, YH, TSu and RA contributed to acquisition of the data. SV, EW, SI and GI drafted and revised the manuscript. All authors read and approved the final manuscript.

Acknowledgments

The authors thank Ms. Kotomi Toriumi, Ms. Haruka Yonekura and Ms. Satoko Arai for the excellent secretarial supports.

References

1. Cheng R, Feng F, Meng F, Deng C, Feijen J, and Zhong Z: **Glutathione-responsive nano-vehicles as a promising platform for targeted intracellular drug and gene delivery.** *J Control Release* 2011, **152**: 2-12.
2. Huang C, Neoh KG, Wang L, Kang ET, and Shuter B: **Surface functionalization of superparamagnetic nanoparticles for the development of highly efficient magnetic resonance probe for macrophages.** *Contrast Media Mol Imaging* 2011, **6**: 298-307.
3. Pan J, Wan D, and Gong J: **PEGylated liposome coated QDs/mesoporous silica core-shell nanoparticles for molecular imaging.** *Chem Commun (Cambridge)* 2011, **47**: 3442-4.
4. Yildirimer L, Thanh NT, Loizidou M, and Seifalian AM: **Toxicology and clinical potential of nanoparticles.** *Nano Today* 2011, **6**: 585-607.
5. Napierska D, Thomassen LC, Lison D, Martens JA, and Hoet PH: **The nanosilica hazard: Another variable entity.** *Part Fibre Toxicol* 2010, **7**: 39.
6. Murugadoss S, Lison D, Godderis L, Van Den Brule S, Mast J, Brassinne F, Sebaihi N, and Hoet PH: **Toxicology of silica nanoparticles: An update.** *Arch Toxicol* 2017, **91**: 2967-3010.
7. Hansen SF, Michelson ES, Kamper A, Borling P, Stuer-Lauridsen F, and Baun A: **Categorization framework to aid exposure assessment of nanomaterials in consumer products.** *Ecotoxicology* 2008, **17**: 438-47.
8. Kempen PJ, Greasley S, Parker KA, Campbell JL, Chang HY, Jones JR, Sinclair R, Gambhir SS, and Jokerst JV: **Theranostic mesoporous silica nanoparticles biodegrade after pro-survival drug delivery and ultrasound/magnetic resonance imaging of stem cells.** *Theranostics* 2015, **5**: 631-42.
9. Hnizdo E, Sullivan PA, Bang KM, and Wagner G: **Association between chronic obstructive pulmonary disease and employment by industry and occupation in the US population: a study of data from the Third National Health and Nutrition Examination Survey.** *Am J Epidemiol* 2002, **156**: 738-46.
10. Ross MH and Murray J: **Occupational respiratory disease in mining.** *Occup Med (Lond)* 2004, **54**: 304-10.

11. Hnizdo E and Vallyathan V: **Chronic obstructive pulmonary disease due to occupational exposure to silica dust: a review of epidemiological and pathological evidence.** *Occup Environ Med* 2003, **60**: 237-43.
12. Yu Y, Duan J, Yu Y, Li Y, Liu X, Zhou X, Ho KF, Tian L, and Sun Z: **Silica nanoparticles induce autophagy and autophagic cell death in HepG2 cells triggered by reactive oxygen species.** *J Hazard Mater* 2014, **270**: 176-86.
13. Fedeli C, Selvestrel F, Tavano R, Segat D, Mancin F, and Papini E: **Catastrophic inflammatory death of monocytes and macrophages by overtaking of a critical dose of endocytosed synthetic amorphous silica nanoparticles/serum protein complexes.** *Nanomedicine (Lond)* 2013, **8**: 1101-26.
14. Ahmad J, Ahamed M, Akhtar MJ, Alrokayan SA, Siddiqui MA, Musarrat J, and Al-Khedhairy AA: **Apoptosis induction by silica nanoparticles mediated through reactive oxygen species in human liver cell line HepG2.** *Toxicol Appl Pharmacol* 2012, **259**: 160-8.
15. Nemmar A, Yuvaraju P, Beegam S, Yasin J, Dhaheri RA, Fahim MA, and Ali BH: **In vitro platelet aggregation and oxidative stress caused by amorphous silica nanoparticles.** *Int J Physiol Pathophysiol Pharmacol* 2015, **7**: 27-33.
16. Maser E, Schulz M, Sauer UG, Wiemann M, Ma-Hock L, Wohlleben W, Hartwig A, and Landsiedel R: **In vitro and in vivo genotoxicity investigations of differently sized amorphous SiO2 nanomaterials.** *Mutat Res Genet Toxicol Environ Mutagen* 2015, **794**: 57-74.
17. Dostert C, Petrilli V, Van Bruggen R, Steele C, Mossman BT, and Tschopp J: **Innate immune activation through Nalp3 inflammasome sensing of asbestos and silica.** *Science* 2008, **320**: 674-7.
18. Rubio L, Pyrgiotakis G, Beltran-Huarac J, Zhang Y, Gaurav J, Deloid G, Spyrogianni A, Sarosiek KA, Bello D, and Demokritou P: **Safer-by-design flame-sprayed silicon dioxide nanoparticles: the role of silanol content on ROS generation, surface activity and cytotoxicity.** *Part Fibre Toxicol* 2019, **16**: 40.
19. Kusaka T, Nakayama M, Nakamura K, Ishimiya M, Furusawa E, and Ogasawara K: **Effect of silica particle size on macrophage inflammatory responses.** *PLoS One* 2014, **9**: e92634.
20. Morris AS, Adamcakova-Dodd A, Lehman SE, Wongrakpanich A, Thorne PS, Larsen SC, and Salem AK: **Amine modification of nonporous silica nanoparticles reduces inflammatory response following intratracheal instillation in murine lungs.** *Toxicol Lett* 2016, **241**: 207-15.
21. Marzaioli V, Aguilar-Pimentel JA, Weichenmeier I, Luxenhofer G, Wiemann M, Landsiedel R, Wohlleben W, Eiden S, Mempel M, Behrendt H, Schmidt-Weber C, Gutermuth J, and Alessandrini F: **Surface modifications of silica nanoparticles are crucial for their inert versus proinflammatory and immunomodulatory properties.** *Int J Nanomedicine* 2014, **9**: 2815-32.
22. Brandenberger C, Rowley NL, Jackson-Humbles DN, Zhang Q, Bramble LA, Lewandowski RP, Wagner JG, Chen W, Kaplan BL, Kaminski NE, Baker GL, Worden RM, and Harkema JR: **Engineered silica nanoparticles act as adjuvants to enhance allergic airway disease in mice.** *Part Fibre Toxicol* 2013, **10**: 26.
23. Han B, Guo J, Abrahaley T, Qin L, Wang L, Zheng Y, Li B, Liu D, Yao H, Yang J, Li C, Xi Z, and Yang X: **Adverse effect of nano-silicon dioxide on lung function of rats with or without ovalbumin**

immunization. *PLoS One* 2011, **6**: e17236.

24. Park HJ, Sohn JH, Kim YJ, Park YH, Han H, Park KH, Lee K, Choi H, Um K, Choi IH, Park JW, and Lee JH: **Acute exposure to silica nanoparticles aggravate airway inflammation: Different effects according to surface characteristics.** *Exp Mol Med* 2015, **47**: e173.
25. Han H, Park YH, Park HJ, Lee K, Um K, Park JW, and Lee JH: **Toxic and adjuvant effects of silica nanoparticles on ovalbumin-induced allergic airway inflammation in mice.** *Respir Res* 2016, **17**: 60.
26. Bagwe RP, Hilliard LR, and Tan W: **Surface modification of silica nanoparticles to reduce aggregation and nonspecific binding.** *Langmuir* 2006, **22**: 4357-62.
27. Marzaioli V, Gross CJ, Weichenmeier I, Schmidt-Weber CB, Gutermuth J, Gross O, and Alessandrini F: **Specific surface modifications of silica nanoparticles diminish inflammasome activation and in vivo expression of selected inflammatory genes.** *Nanomaterials (Basel)* 2017, **7**.
28. Lankoff A, Arabski M, Wegierek-Ciuk A, Kruszewski M, Lisowska H, Banasik-Nowak A, Rozga-Wijas K, Wojewodzka M, and Slomkowski S: **Effect of surface modification of silica nanoparticles on toxicity and cellular uptake by human peripheral blood lymphocytes in vitro.** *Nanotoxicology* 2013, **7**: 235-50.
29. Morishige T, Yoshioka Y, Inakura H, Tanabe A, Yao X, Narimatsu S, Monobe Y, Imazawa T, Tsunoda S, Tsutsumi Y, Mukai Y, Okada N, and Nakagawa S: **The effect of surface modification of amorphous silica particles on NLRP3 inflammasome mediated IL-1beta production, ROS production and endosomal rupture.** *Biomaterials* 2010, **31**: 6833-42.
30. Agency EUSEP, *Air Quality Criteria for Particulate Matter Volume II*. 2004, Environmental Protection Agency: Washington, DC.
31. Knust J, Ochs M, Gundersen HJ, and Nyengaard JR: **Stereological estimates of alveolar number and size and capillary length and surface area in mice lungs.** *Anat Rec (Hoboken)* 2009, **292**: 113-22.
32. Fleming TJ, Fleming ML, and Malek TR: **Selective expression of Ly-6G on myeloid lineage cells in mouse bone marrow. RB6-8C5 mAb to granulocyte-differentiation antigen (Gr-1) detects members of the Ly-6 family.** *J Immunol* 1993, **151**: 2399-408.
33. Hestdal K, Ruscetti FW, Ihle JN, Jacobsen SE, Dubois CM, Kopp WC, Longo DL, and Keller JR: **Characterization and regulation of RB6-8C5 antigen expression on murine bone marrow cells.** *J Immunol* 1991, **147**: 22-8.
34. Vranic S, Gosens I, Jacobsen NR, Jensen KA, Bokkers B, Kermanizadeh A, Stone V, Baeza-Squiban A, Cassee FR, Tran L, and Boland S: **Impact of serum as a dispersion agent for in vitro and in vivo toxicological assessments of TiO2 nanoparticles.** *Arch Toxicol* 2017, **91**: 353-363.
35. Tada-Oikawa S, Eguchi M, Yasuda M, Izuoka K, Ikegami A, Vranic S, Boland S, Tran L, Ichihara G, and Ichihara S: **Functionalized surface-charged SiO2 nanoparticles induce pro-inflammatory responses, but are not lethal to Caco-2 cells.** *Chem Res Toxicol* 2020, **33**: 1226-1236.
36. Aman J, van der Heijden M, van Lingen A, Girbes AR, van Nieuw Amerongen GP, van Hinsbergh VW, and Groeneveld AB: **Plasma protein levels are markers of pulmonary vascular permeability and degree of lung injury in critically ill patients with or at risk for acute lung injury/acute respiratory distress syndrome.** *Crit Care Med* 2011, **39**: 89-97.

Figures

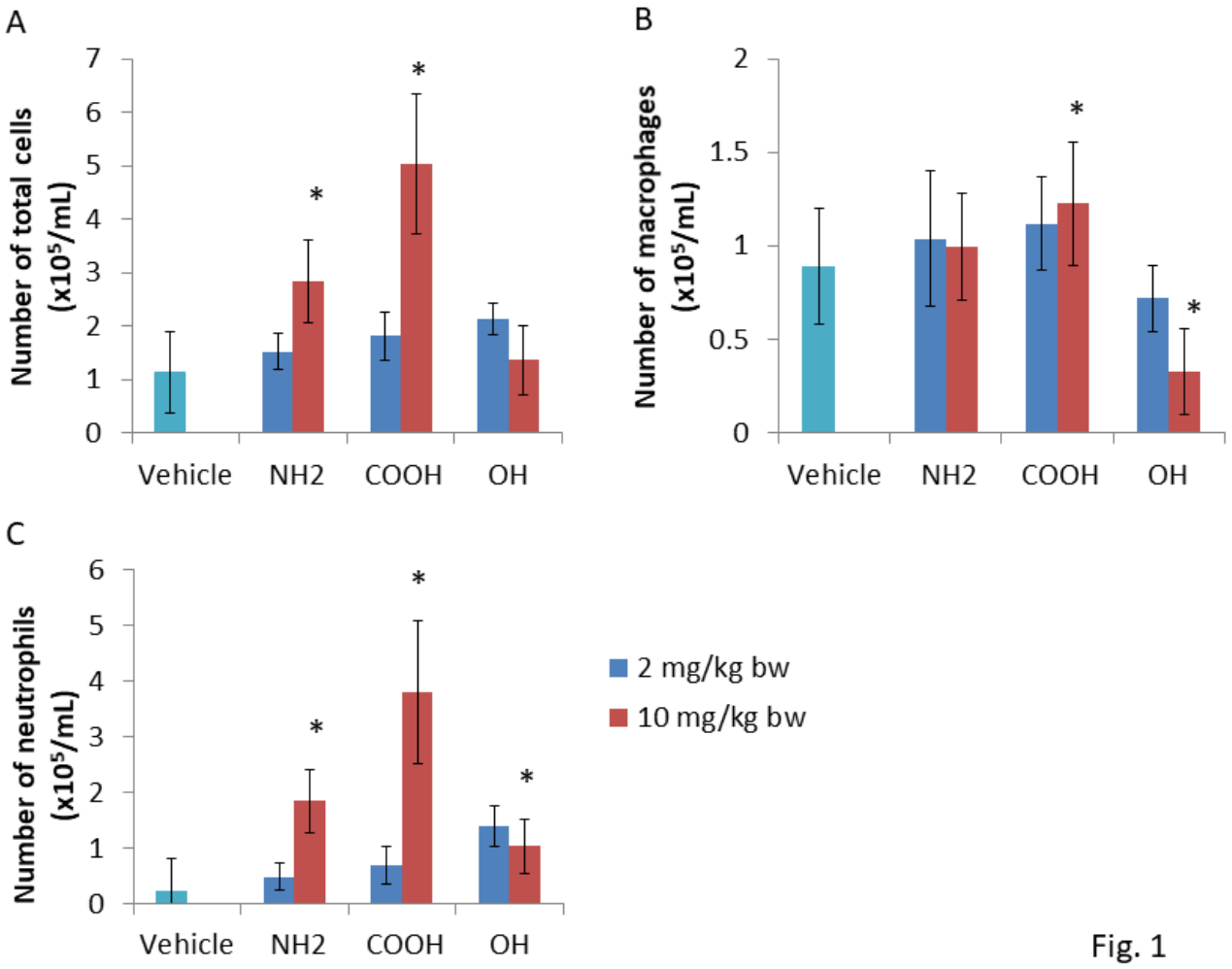

Figure 1

Total and differential cell count in BALF of mice exposed to SiO2 NPs for 24 h via pharyngeal aspiration. Animals received OH-, COOH- or NH2- modified rhodamine-labeled SiO2 NPs at 2 or 10 mg/kg bw by pharyngeal aspiration. At 24 h after the treatment, BALF was collected and total and differential cell counts were determined using Differential Quick Stain Kit and hematocell counter. About 400 cells in three fields were counted on a slide from one animal each. Data are mean±SD (n=6 each). A) Total cell count. B) Macrophage cell count. C) Neutrophil cell count BALF. *P<0.05, compared with the vehicle group, by Dunnett's multiple comparison following ANOVA.

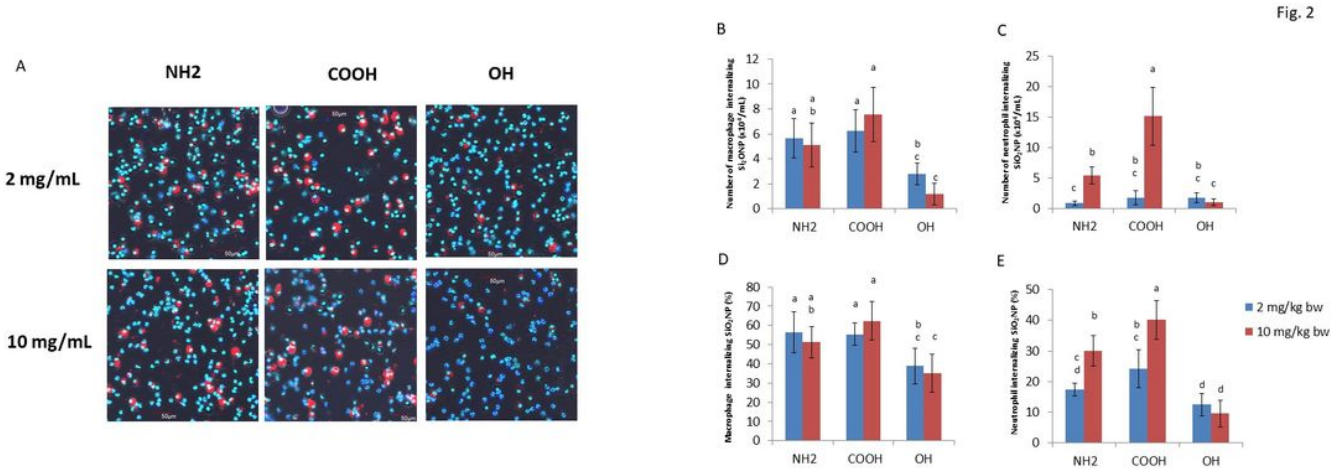

Figure 2

SiO2 NPs with macrophages and neutrophils recovered from BALF. Mice were treated with OH-, NH2- or COOH- modified rhodamine labelled SiO2 NPs at 2 or 10 mg/kg bw by pharyngeal aspiration. At 24 h after the treatment, BALF was collected and cytospinned on slides. A) Confocal images of the cells recovered from BALF and stained using Differential Quick Stain Kit. Rohdamine-labelled SiO2 NPs are stained red, while the nuclei and cytoplasm are stained dark blue and light blue, respectively. Scale bars = 50 μm. B) Count of macrophages with internalized rhodamine-labelled SiO2NPs. About 400 cells in three fields were counted on a slide from each animal. *P<0.05, compared with the vehicle group, by Tukey multiple comparison following ANOVA. Groups with different letters indicate significant difference between them. C) Counts of neutrophils with internalized rhodamine-labelled SiO2 NPs. About 400 cells in three fields were counted on a slide from each animal. *P<0.05, compared with the vehicle group, by Tukey multiple comparison following ANOVA. Groups with different letters indicate significant difference between them. (D) Percentage of the macrophages with internalized NPs relative to the total number of macrophages. (E) Percentage of neutrophils with internalized NPs relative to the total neutrophils.

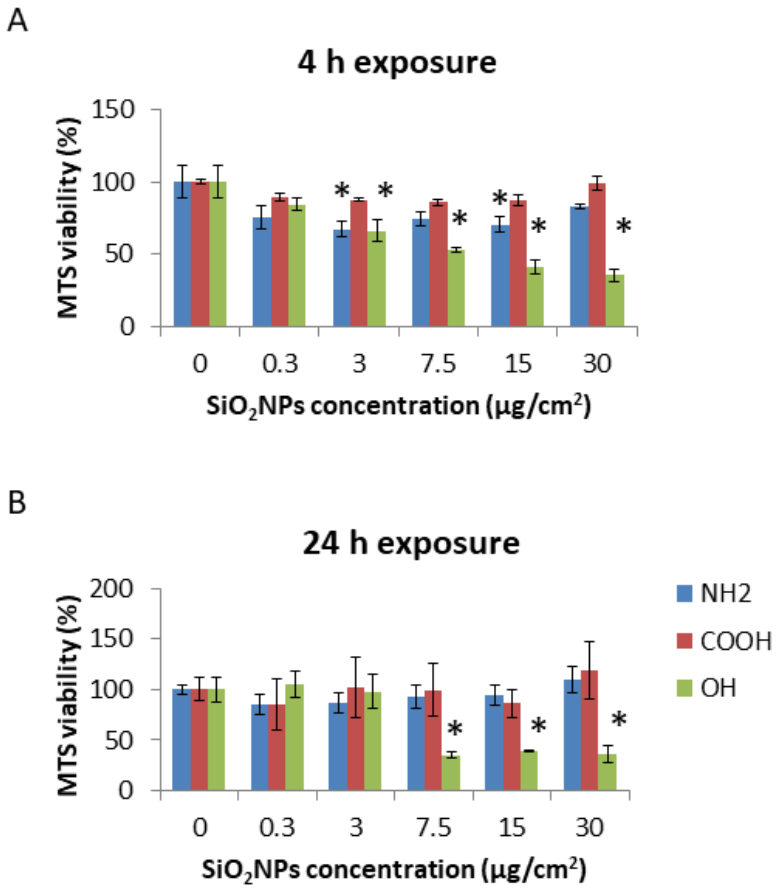

Fig. 3

Figure 3

Viability of RAW264.8 cells, as determined by MTS, at 4 or 24 h after treatment with SiO2 NPs at the indicated concentrations. Cells were treated with OH-, NH2 or COOH-modified Rohdamine-labelled SiO2 NPs dispersed in the cell culture medium at 0.3 to 30 µg/cm2 (1-100 µg/mL). After the treatment, cell viability was assessed by measuring absorbance at 490 nm, which reflected the reduction of {3-(4,5-dimethylthiazol-2-yl)-5-(3-carboxymethoxyphenyl)-2-(4-sulfophenyl)-2H-tetrazolium} (MTS) to formazan by mitochondria in viable cells. Data are plotted as average±SD (n = 6). *P<0.05, compared with untreated control (0 µg/mL), by Dunnett's test following ANOVA.

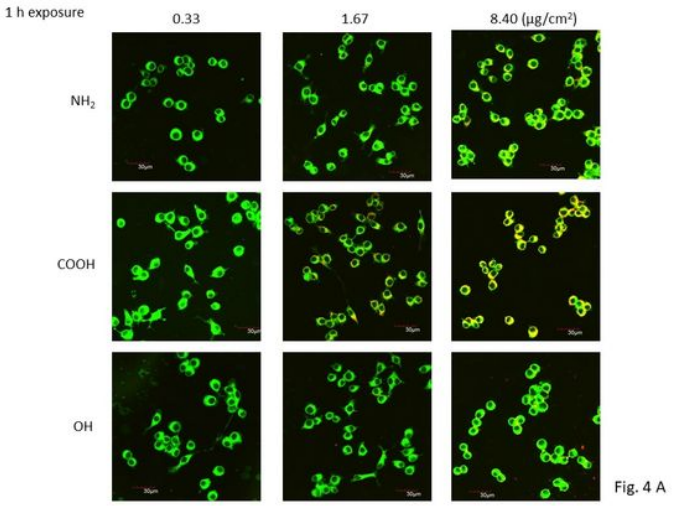

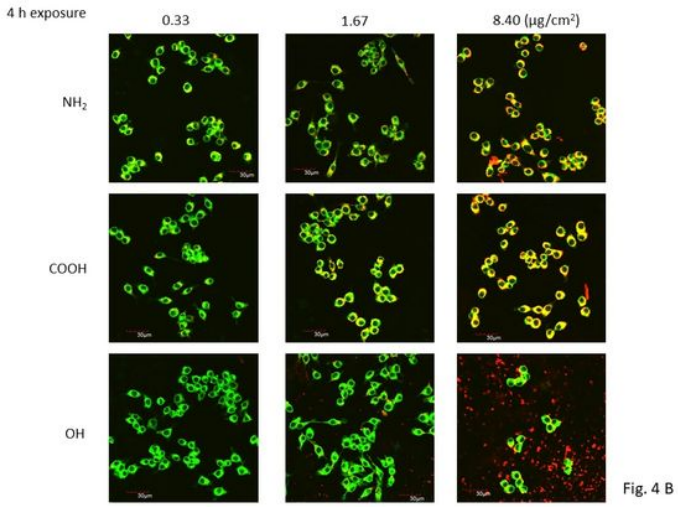

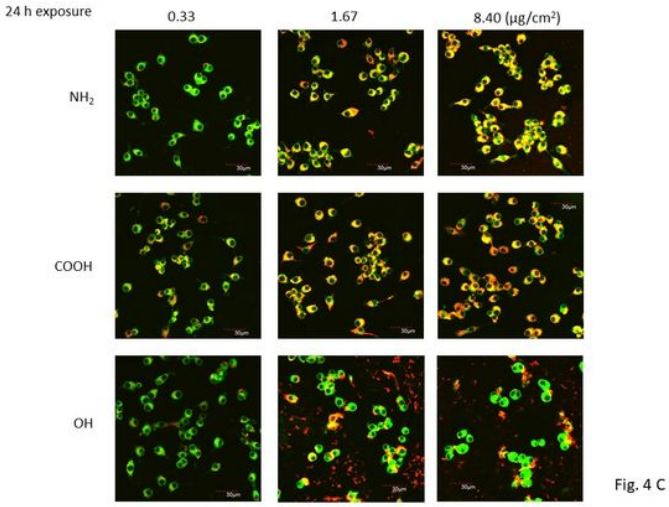

Figure 4

Interaction of SiO2 NPs with RAW264.8 macrophages. A) RAW 264.8 cells were exposed to different concentrations of three types of SiO2 NPs for 1 hour. B) RAW 264.8 cells were exposed to different concentrations of three types of SiO2 NPs for 4 hours. C) RAW 264.8 cells were exposed to different concentrations of three types of SiO2 NPs for 24 hours. Interaction of NPs with cells was assessed by confocal microscopy. Green – plasma membrane, red – SiO2 NPs. Scale bars = 30 µm.

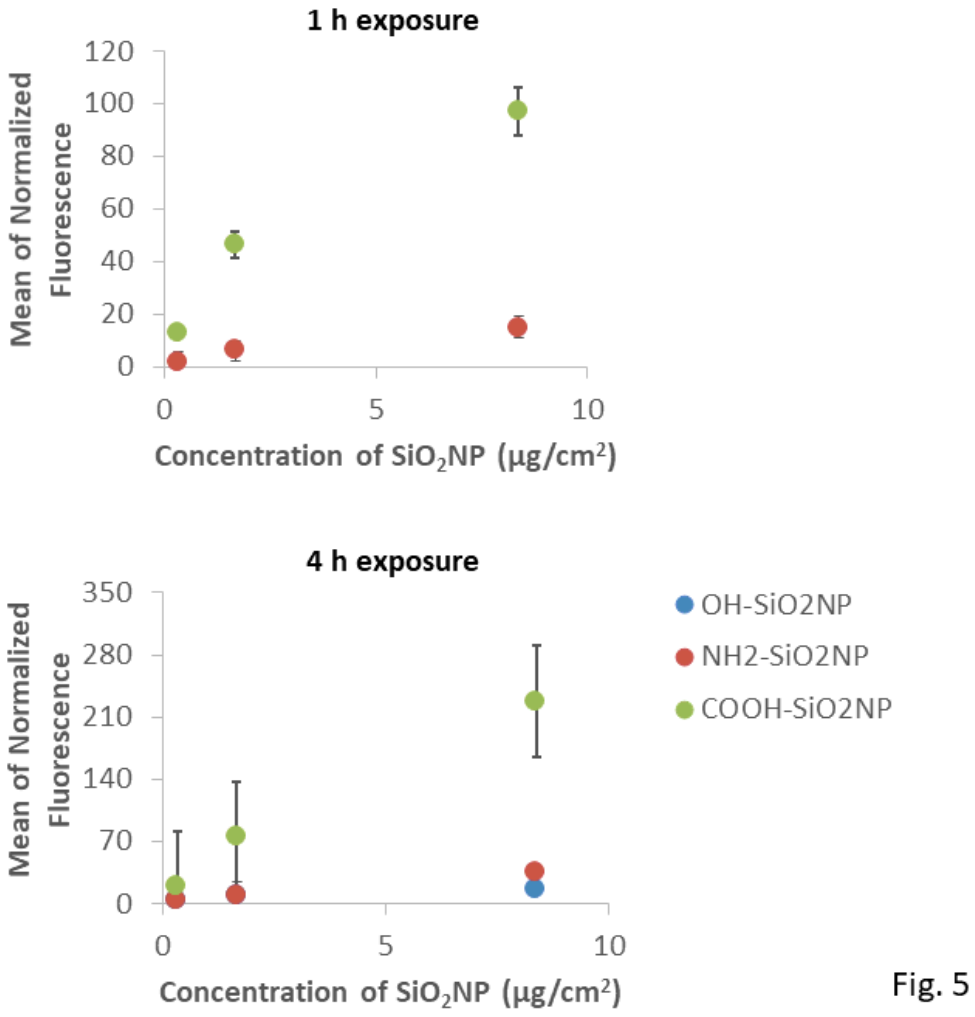

Figure 5

Assessment of internalization of SiO2 NPs into RAW264.8 cells by flow cytometry. Cells were exposed to different concentrations of NPs for 1h or 4. After the treatment, they were washed and incubated with 0.1% trypan blue for 1 min, in order to quench fluorescence emanating from NPs adsorbed on the surface of the cells. Mean fluorescence intensity of the cells was analyzed using excitation/emission wavelengths set corresponding to rhodamine dye. Data are MFI±SD (n = 3, 10,000 cells were analyzed per sample).

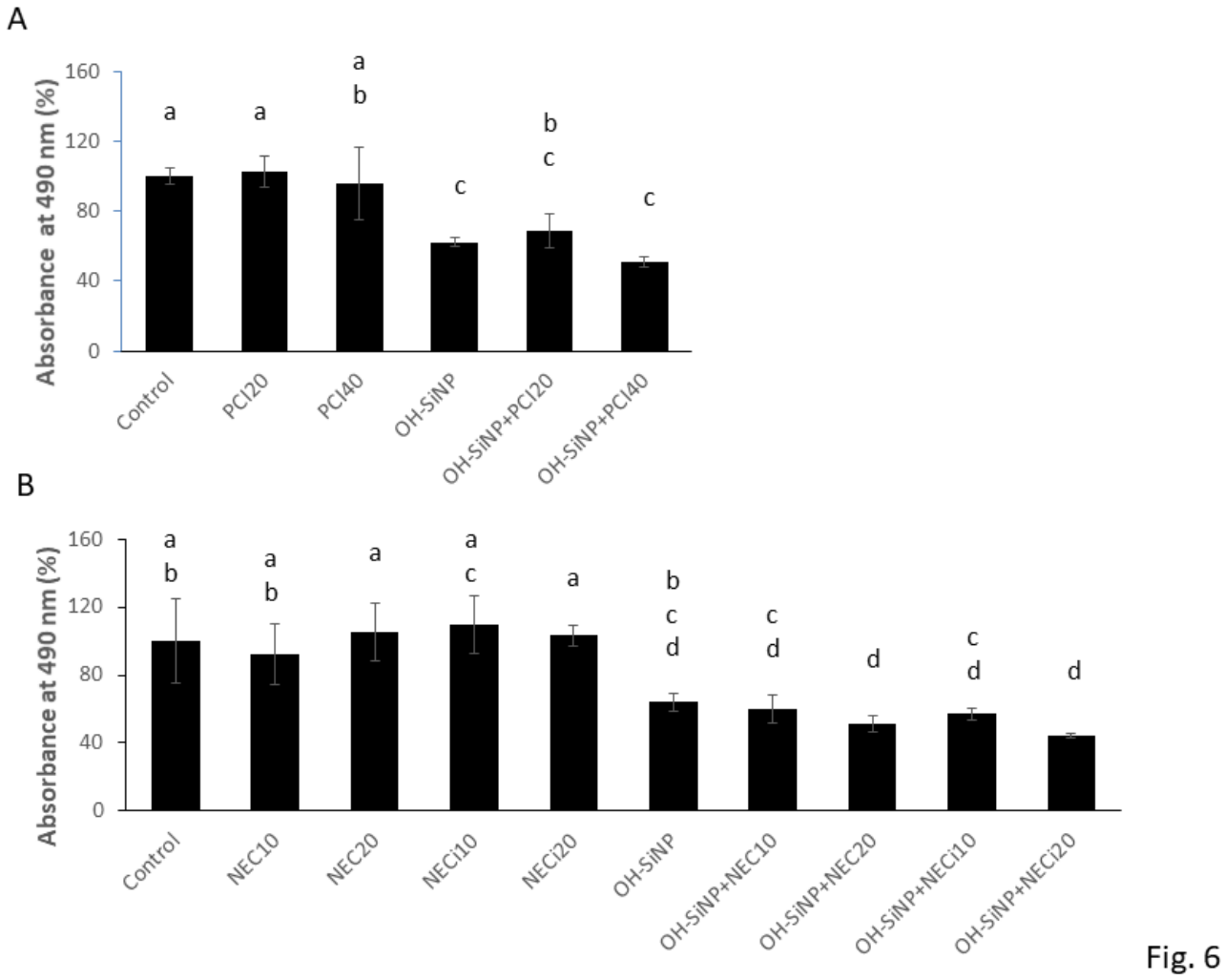

Fig. 6

Figure 6

Effect of pan-caspase inhibitor and necroptosis inhibitor on MTS cytotoxicity of OH-SiO2 NPs in vitro. A) Effect of pan-caspase inhibitor Z-VAD-FMK on MTS viability of cells exposed to OH-SiO2 NPs. RAW264.1 cells were preincubated with 20 or 40 μM of pan-caspase inhibitor Z-VAD-FMK or vehicle for one hour, and exposed to OH-SiO2 NPs at 8.40 μg /cm2 (28 μg/mL) for 18 hours. Cytotoxicity was evaluated using CellTiter 96® Aqueous One Solution Cell Proliferation Assay (Promega, Madison, WI). PCI20: pan caspase inhibitor 20 μM, PCI40: pan caspase inhibitor 40μM, OH-SiNP:OH-SiO2 NPs. B) Effect of necroptosis inhibitor necrostatin-1 on MTS viability of cells exposed to OH-SiO2 NPs. RAW264.1 cells were preincubated with necrostatin-1 or necrostatin-1 inactive control at 10 or 20 μM for one hour, and exposed to OH-SiO2 NPs at 8.40 μg /cm2 (28 μg/mL) for 18 hours. Cytotoxicity was evaluated using CellTiter 96® Aqueous One Solution Cell Proliferation Assay (Promega, Madison, WI). NEC10: necrostatin-1 10 μM, NEC20: necrostatin-1 10 μM, NECi10:necrostatin-1 inactive control 10 μM, NECi20: necrostatin-1 inactive control 20 μM. Different letters indicate statistical difference between groups by Tukey's multiple comparison following ANOVA. Significance level is 0.05.

Supplementary Files

This is a list of supplementary files associated with this preprint. Click to download.

- Supplementary1.TIF
- Supplementary2.TIF
- Supplementary3.TIF
- Supplementary4.TIF
- Supplementary5.TIF